



ELSEVIER

Biochimica et Biophysica Acta 1500 (2000) 257–264

BIOCHIMICA ET BIOPHYSICA ACTA

BBAwww.elsevier.com/locate/bba

Caldesmon and heat shock protein 20 phosphorylation in nitroglycerin- and magnesium-induced relaxation of swine carotid artery

Christopher M. Rembold *, Matthew O'Connor

Cardiovascular Division, Departments of Internal Medicine and Physiology, University of Virginia Health System, Charlottesville, VA 22908, USA

Received 12 August 1999; received in revised form 29 November 1999; accepted 29 November 1999

Abstract

Nitrovasodilators, high extracellular Mg^{2+} , and some other relaxing agents can cause smooth muscle relaxation without reductions in myosin regulatory light chain (MRLC) phosphorylation. Relaxations without MRLC dephosphorylation suggest that other regulatory systems, beyond MRLC phosphorylation, are present in smooth muscle. We tested whether changes in caldesmon phosphorylation, heat shock protein 20 (HSP20) phosphorylation, or intracellular pH (pH_i) could be responsible for relaxation without MRLC dephosphorylation. In unstimulated tissues, caldesmon was phosphorylated 1.02 ± 0.10 mol P_i /mol caldesmon (mean \pm 1 S.E.M.), HSP20 was phosphorylated 0.005 ± 0.003 mol P_i /mol HSP20, and estimated pH_i was 7.21 ± 0.07 . Histamine stimulation induced a contraction, an intracellular acidosis, but did not significantly change caldesmon or HSP20 phosphorylation. Addition of nitroglycerin induced a relaxation, significantly increased HSP20 phosphorylation to 0.18 ± 0.02 mol P_i /mol HSP20, did not significantly change caldesmon phosphorylation, and pH_i returned to near unstimulated values. Increase in extracellular Mg^{2+} to 10 mM induced a relaxation, but did not significantly change HSP20 or caldesmon phosphorylation. These data suggest that changes in caldesmon phosphorylation, HSP20 phosphorylation, or pH_i cannot be the sole explanation for relaxation without MRLC dephosphorylation. However, it is possible that HSP20 phosphorylation may be involved in nitroglycerin-induced relaxation without MRLC dephosphorylation. © 2000 Elsevier Science B.V. All rights reserved.

Keywords: Caldesmon; Calcium ion concentration; Intracellular pH; Vascular smooth muscle

1. Introduction

Most excitatory stimuli induce smooth muscle contraction by increasing myoplasmic Ca^{2+} concentration, formation of the $4Ca^{2+}$ -calmodulin-myosin light chain kinase (MLCK) complex, and phosphorylation of Ser¹⁹ in the myosin regulatory light chains

(MRLC) [1]. In most cases, smooth muscle relaxation is felt to be the reversal of this process: reduction in Ca^{2+} , inhibition of MLCK, and MRLC dephosphorylation [2].

There are several agents that cause greater relaxation than predicted by reductions in MRLC phosphorylation. Typically, these relaxing agents decrease force to near resting values, while MRLC phosphorylation only decreases modestly to a value still significantly greater than resting values. Such relaxations include the responses to activators of guanylyl cyclase, such as NO or inhibitors of phosphodiester-

* Corresponding author. Box 146, Cardiovascular Division, University of Virginia Health System, Charlottesville, VA 22908, USA. Fax: +1-804-924-9604; E-mail: crembold@virginia.edu

ases that elevate cellular [cGMP] [3–6]. Other situations are treatment with okadaic acid, a non-specific phosphatase inhibitor [7], some Ca^{2+} depletion protocols [8,9], some Ca^{2+} channel blockers [10], high extracellular Mg^{2+} [11], and other combinations of excitatory and inhibitory stimuli [12]. This phenomenon has been studied mostly in vascular smooth muscle; however, it is most dramatic in tissues, such as the corpus cavernosum, where inhibitory innervation is a key physiological control mechanism [6].

One potential reason for relaxation without MRLC dephosphorylation is that the MRLC could be phosphorylated on a different amino acid residue. However, we found that MRLC phosphorylation during relaxation with nitroglycerin [3] and or high extracellular magnesium [11] induced relaxation was all on Ser¹⁹, suggesting that MRLC phosphorylation at inactive sites cannot explain uncoupling of force from MRLC phosphorylation.

Relaxations without MRLC dephosphorylation suggest that MRLC phosphorylation is not the only determinant of activation and cross-bridge cycling in smooth muscle, but do not establish the importance or the physiological role of a Ca^{2+} -independent regulatory mechanism.

There are other candidate regulatory systems for force in smooth muscle (reviewed in [13]): (1) the thin filament proteins caldesmon and calponin can alter thin filament function; (2) myosin can both bind Ca^{2+} (at a low affinity) and be phosphorylated on the heavy chain; (3) phorbol diesters, presumably by activation of protein kinase C, can induce contraction by an unknown cascade; (4) some investigators propose non-crossbridge mediated stress in the form of cytoskeletal domain crosslinks; (5) changes in intracellular pH (pH_i) have been reported to alter the relation between Ca^{2+} and contraction [14,15]; and finally, (6) phosphorylation of heat shock protein 20 (HSP20) has been found to correlate with cyclic nucleotide-induced relaxation [16].

In this study, we evaluated three potential force regulatory systems to determine whether they could have a role in relaxation without MRLC dephosphorylation. We studied the role of caldesmon phosphorylation, HSP20 phosphorylation, and pH_i during relaxation induced by nitroglycerin or high extracellular magnesium. We previously showed

that these agents induce relaxation without MRLC dephosphorylation [3,11].

2. Materials and methods

2.1. Tissues

Swine common carotid arteries were obtained from a slaughterhouse and transported at 0°C in physiological salt solution (PSS). PSS contained (mM): NaCl, 140; KCl, 4.7; 3-[*N*-morpholino] propane sulfonic acid (MOPS) 5; Na_2HPO_4 , 1.2; CaCl_2 , 1.6; MgSO_4 , 1.2; D-glucose, 5.6; pH adjusted to 7.4 at 37°C. Dissection of medial strips, mounting and determination of the optimum length for stress development at 37°C was performed as described. [17]. The intimal surface was mechanically rubbed to remove the endothelium.

2.2. ³²P-Labeling of intact tissues

Tissues were prepared and mounted as described above. Tissues were placed in PO_4 -free PSS and incubated with ³²P_i (³²P-orthophosphate) 300 μCi/strip (0.18 mCi/ml) for 4–5 h at 37°C. Tissues were rinsed and stretched for 1 h, subjected to treatments, and frozen in dry ice/acetone slurry as described [18]. Frozen tissues were split into two pieces: one for caldesmon extraction and the other for determination of the radiospecific activity of tissue [γ -³²P]ATP.

2.3. Measurement of caldesmon phosphorylation

This procedure was modified from that described by Dr. Len Adam [19]. Half of the tissue was homogenized on ice in 0.4 ml of homogenization buffer containing (in mM) Tris, 25 (pH 8.8); Na-pyrophosphate, 100; NaCl, 250; EGTA, 10; EDTA, 5, NaF, 50; NP-40, 0.1%; DTT, 0.01; and PMSF, 0.001. The homogenates were centrifuged for 2 min at 14 000 × *g*. The supernatant was boiled for 10 min and centrifuged again for 2 min at 14 000 × *g*. The supernatant was diluted 1:10 in equilibration buffer containing (mM) MOPS, 20 (pH 7.0); EDTA, 1; EGTA, 1; and DTT, 1. The diluted supernatant was then applied to a 0.5-ml DEAE-Sephacel column (Sigma, I-6505). The columns were washed with 1.2

ml equilibration buffer and then 1.2 ml 0.15 M NaCl. For Fig. 1 the caldesmon was then eluted with increasing concentrations of NaCl as described. Since the caldesmon eluted with 0.2–0.3 M NaCl, we eluted caldesmon in all other experiments with 1 ml of 0.3 M NaCl after washing with 0.15 M NaCl. The elution was run on a 12% SDS PAGE gel, stained with Coomassie blue and ^{32}P activity determined by cutting out the caldesmon bands and scintillation counting. The amount of protein was determined by comparison with caldesmon standards loaded on the gel.

2.4. ATP specific activity determination

The remaining portion of the ^{32}P -labeled tissue was homogenized in 0.2 ml 10% trichloroacetic acid at 4°C, centrifuged and the supernatant washed three times with ether at 4°C as described [18]. The sample was lyophilized and resuspended in 30 μl water. Aliquots were incubated in 100 mM Tris buffer pH 8.0 (at 30°C); 5 mM MgCl_2 ; 2 mM dithiothreitol; containing 2 mg/ml phosphorylase *b*, 0.1 mg/ml phosphorylase kinase. Aliquots were taken at 30 min, spotted on cellulose filter paper and immersed in cold 10% trichloroacetic acid; 4% disodium pyrophosphate. Filters were washed four times with TCA, each 10 min; washed once each in 95% ethanol, ethyl ether, dried and radioactivity measured by liquid scintillation spectrometry. Sample specific activities were determined by comparison with a standard curve derived from samples of known [^{32}P]ATP specific activities that were assayed under the same conditions. Preliminary studies established that the reaction had proceeded to completion by 30 min. Stoichiometry of caldesmon phosphorylation (mol P_i /mol caldesmon) was calculated by multiplying the dpm/ μg caldesmon by the MW of caldesmon ($\mu\text{g}/\mu\text{mol}$) and then dividing by the specific activity of [γ - ^{32}P]ATP (dpm/ μmol [γ - ^{32}P]ATP) [18].

2.5. Measurement of HSP20 phosphorylation

Swine carotid arteries were pharmacologically treated and frozen in an acetone dry ice slurry [17]. After air drying, the tissues were homogenized a buffer containing 1% SDS, 10% glycerol, and 20 mM dithiothreitol. Full strength, half strength, and quarter-strength dilutions of samples were then sep-

arated on one-dimensional isoelectric focusing (pI 5–8), blotted to nitrocellulose, immunostained with a rabbit polyclonal anti-HSP20 antibody, and detected with enhanced chemiluminescence. The dilutions ensured that the enhanced chemiluminescence detection system was in the linear range. We made anti-HSP20 antibody by injecting rabbits with gel purified recombinant HSP20 (sequence confirmed by mass spectroscopy).

2.6. Intracellular pH measurement

Intracellular pH was measured with BCECF loaded intracellularly by incubation of dissected tissues in the acetomethoxy ester of BCECF (BCECF-AM, Molecular Probes, Eugene, OR) [20]. The final loading solution was MOPS PSS containing 4 μM BCECF-AM, 0.133 mg/ml Pluronic F127, and 0.66% dimethylsulfoxide. Arterial strips were loaded at 37°C for 1 h and washed in PSS for 1–1.5 h before each experiment. The experimental apparatus consisted of a Nikon xenon light source, the output of which was directed through a rotating filter wheel that had 436 ± 13 nm and 485 ± 12 nm filters rotating at 3000 rpm. Excitation light passed through one arm of a bifurcated light guide, which was placed 0.5–1 mm from the luminal surface of the smooth muscle tissue. The tissue was isometrically mounted to a Harvard Bioscience capacitive force transducer and bathed in a 3-ml jacketed tissue bath. The second arm of the bifurcated light guide passed emission light through a 530 ± 15 nm filter to a photomultiplier tube. Fluorescence signals were electronically demultiplexed and the force, 436 and 485 fluorescence signals were converted to digital signals and stored on a personal computer.

2.7. Calibration of BCECF signals

After completing pharmacological manipulations, tissues were incubated in a calibration solution containing 3 μM nigericin, KCl, 145; MOPS, 5; CaCl_2 , 1.6; MgSO_4 , 1.2; D-glucose, 5.6; EDTA, 0.02; pH adjusted to 6.8 or 7.4 at 37°C (this solution has no added Na^+) and a two point calibration performed at 7.4 and 6.8 as described [20]. We found that the relationship between pH_o and the 485/436 ratio was linear between pH 6.6 and 7.8 ($n = 5$). Calculated pH_i

estimates are approximate because: (1) some photobleaching and dye leakage occurred during the experiment; (2) nigericin may not totally equilibrate the pH gradient in all cells; and (3) protein binding can alter the fluorescent properties of BCECF[21]. We were interested in the effects of changes in pH_i ; therefore, signals are reported as change in pH_i rather than absolute pH_i . This normalization decreased variability caused exclusively by differences in estimates of basal pH_i .

2.8. Statistics

Phosphorylation, BCECF signals, and force were compared with an ANOVA with Newman–Keuls tests for individual comparisons. Significance was defined as $P < 0.05$.

3. Results

Caldesmon is a thin filament protein. Caldesmon has both actin and myosin binding domains and appears to weakly tether myosin and actin [22]. Despite this tethering action, binding of caldesmon to actin decreases binding of myosin to actin and decreases myosin's actin activated ATPase activity [22,23]. Caldesmon can be phosphorylated up to 2 mol P_i/mol

caldesmon. Dephosphorylated caldesmon is a more potent inhibitor of myosin's actin activated ATPase than phosphorylated caldesmon [24] although this effect appears dependent on solution composition [22]. There are three reports detailing caldesmon phosphorylation in smooth muscle; all are in swine carotid artery. High $[\text{K}^+]_o$ [25], phorbol dibutyrate [25], endothelin [19], and angiotensin II [19] all increased caldesmon phosphorylation (measured 60 min after stimulation). With high $[\text{K}^+]_o$ stimulation, the time course of changes in caldesmon phosphorylation was slower than the time course of contraction and relaxation [25]. Sustained angiotensin II stimulation was associated with a sustained increase in caldesmon phosphorylation despite the decrease in force associated with tachyphylaxis [19]. Another group found no change in caldesmon phosphorylation with high $[\text{K}^+]_o$, histamine, or norepinephrine stimulation [26]. These studies suggest that caldesmon phosphorylation does not simply correlate with contraction, i.e. (1) caldesmon phosphorylation changed slower than force during high $[\text{K}^+]_o$ contraction/relaxation cycles; and (2) caldesmon phosphorylation remained elevated despite tachyphylaxis with angiotensin II.

We measured caldesmon phosphorylation in $^{32}\text{PO}_4$ -loaded swine carotid arterial tissues [27]. Briefly, tissues were homogenized, boiled, and pro-

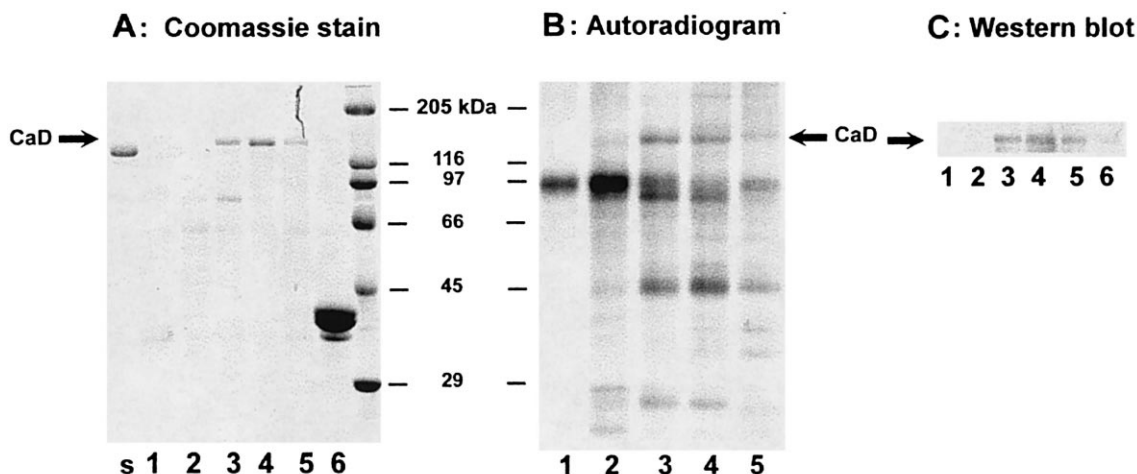


Fig. 1. Demonstration of caldesmon purification. SDS electrophoresis gels of fractions collected from the DEAE Sephacel columns loaded with homogenates from unstimulated swine carotid artery. (A) A Coomassie blue stained gel showing purified gizzard caldesmon (labeled 's'), fractions 1–6 corresponding to elution from the column with 0.1, 0.15, 0.2, 0.25, 0.3, and 0.35 M NaCl, and molecular weight standards. (B) An autoradiogram of fractions 1–5 (0.1–0.3 M NaCl). (C) A Western blot with anti-caldesmon antibody. The arrows show that caldesmon (CaD) eluted in fractions 3–5 corresponding to 0.2–0.3 M NaCl.

teins present in the supernatant separated by DEAE chromatography and then 1D SDS electrophoresis (protocol from Len Adam, see Section 2). The boiling is a crucial step as it eliminates the majority of cellular proteins that are not heat stable. Fig. 1 shows a SDS gel stained with Coomassie blue, an autoradiogram of a second gel, and a Western blot of a third gel. Caldesmon eluted from the DEAE Sephacel column in the 0.2–0.3 M NaCl fractions (lanes 3–5). Detection by anti-caldesmon antibodies (Fig. 1C) identify these bands as caldesmon. The autoradiogram (Fig. 1B) demonstrates that caldesmon was labeled with $^{32}\text{PO}_4$. Fig. 1A shows that gizzard caldesmon migrated at a similar, but not identical MW, as swine caldesmon. This extraction system was used to measure caldesmon phosphorylation in intact swine carotid.

Caldesmon was phosphorylated 1.02 ± 0.10 mol P_i /mol (mean+1 S.E.M., $n=9$) in unstimulated tissues. Histamine ($3 \mu\text{M}$) stimulation induced a contraction but did not significantly change caldesmon phos-

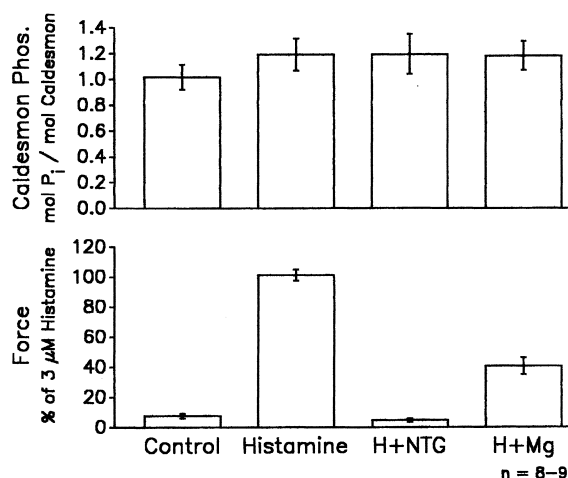


Fig. 2. Lack of a correlation between caldesmon phosphorylation and either contraction or relaxation. Nine sets of swine carotid artery tissues were loaded with $^{32}\text{P}_i$ and then either: (1) not stimulated; (2) stimulated with $3 \mu\text{M}$ histamine alone for 30 min; (3) stimulated with $3 \mu\text{M}$ histamine for 10 min and then relaxed by addition of $10 \mu\text{M}$ nitroglycerin for 20 min (labeled H+NTG); or (4) stimulated with $3 \mu\text{M}$ histamine for 10 min and then relaxed by addition of 10mM Mg^{2+} for 20 min (labeled H+Mg). Contractile force was then measured and the tissues frozen for caldesmon phosphorylation measurement. The bar graph shows that caldesmon phosphorylation was not significantly changed (by Newman–Keuls test) despite significant changes in force. Force was normalized to that observed with $3 \mu\text{M}$ histamine.

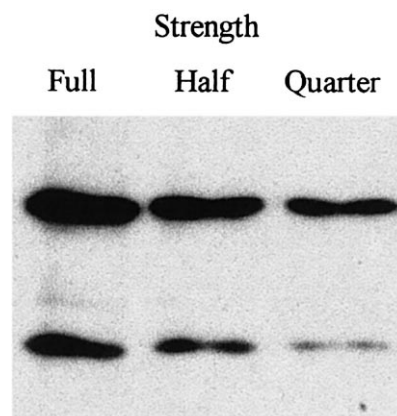


Fig. 3. A representative Western blot of HSP20 immunoreactivity. A tissue (stimulated with $10 \mu\text{M}$ histamine for 10 min and then relaxed by addition of $10 \mu\text{M}$ nitroglycerin for 20 min) was homogenized, proteins separated by isoelectric focusing, immunostained with rabbit anti-HSP20 antibody, and imaged with enhanced chemiluminescence. The upper band is unphosphorylated HSP20 and the lower (more acidic) band is phosphorylated HSP20. The left lane is full-strength homogenate, the center is half-strength, and the right is quarter-strength homogenate.

phorylation. Addition of $10 \mu\text{M}$ nitroglycerin to histamine stimulated tissues induced a significant relaxation, but did not significantly change caldesmon phosphorylation. In histamine-stimulated tissues, increase in extracellular Mg^{2+} to 10mM by addition of MgCl_2 induced a significant relaxation, but did not significantly change caldesmon phosphorylation. These data suggest that alterations in caldesmon phosphorylation cannot be responsible for nitroglycerin- or high extracellular Mg^{2+} -induced relaxation without MRLC dephosphorylation (Fig. 2).

Heat shock protein 20 (HSP20) may have a role in cyclic nucleotide-induced smooth muscle relaxation. The laboratory of Colleen Brophy found that cyclic nucleotide-dependent relaxation was associated with phosphorylation of HSP20 in bovine carotid smooth muscle [16]. HSP20 is highly homologous to the small heat shock proteins αB crystallin and HSP27 [28]. HSP25 (the rat form of HSP27) was first characterized as an inhibitor of actin polymerization [29]. Phosphorylation of HSP27 by p38 MAP kinase increases the stability of actin filaments in cells exposed to cytochalasin D [30]. Antibodies to HSP27 inhibited bombesin-induced contraction of rabbit anal smooth muscle [31]. These data suggest that HSP27, a close relative of HSP20, may be able to

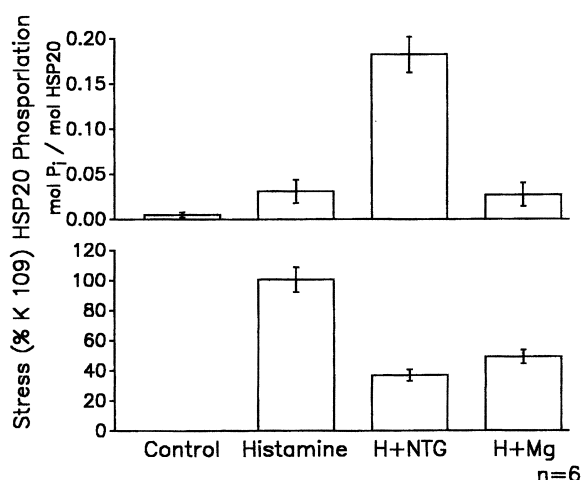


Fig. 4. Correlation between HSP20 phosphorylation with nitroglycerin, but not magnesium-induced relaxation. Six sets of swine carotid artery tissues were: (1) not stimulated; (2) stimulated with 10 μM histamine alone for 30 min; (3) stimulated with 10 μM histamine for 10 min and then relaxed by addition of 10 μM nitroglycerin for 20 min (labeled H+NTG); or (4) stimulated with 3 μM histamine for 10 min and then relaxed by increasing extracellular Mg^{2+} to 10 mM for 20 min (labeled H+Mg). Contractile force was then measured and the tissues frozen for HSP20 phosphorylation measurement. The bar graph shows that HSP20 phosphorylation was significantly increased by treatment with nitroglycerin (by Newman–Keuls test). Both nitroglycerin and magnesium-induced significant relaxations. Force was normalized to that observed previously with 109 mM extracellular K^+ .

regulate contractile proteins. Interestingly, HSP20 contains a cGMP/cAMP-dependent protein kinase consensus phosphorylation site, while HSP27 does not [28]. There are at least two HSP20 isoforms: an acidic form that predominates in swine carotid and a basic form that predominates in urogenital smooth muscle (data not shown). We therefore measured HSP20 phosphorylation in swine carotid artery relaxed with protocols that caused relaxation without MRLC dephosphorylation.

A representative Western blot of HSP20 immunoreactivity from a tissue stimulated with 10 μM histamine for 10 min and then relaxed by addition of 10 μM nitroglycerin for 20 min is shown in Fig. 3. The upper bands are the unphosphorylated acidic isoform of HSP20 and the lower (more acidic) band are phosphorylated acidic isoform of HSP20. The lanes left to right show serial dilutions of homogenate demonstrating that the enhanced chemiluminescence detection system was in its linear range.

HSP20 was phosphorylated 0.005 ± 0.003 mol P_i /mol (mean ± 1 S.E.M., $n = 6$) in unstimulated tissues. Histamine (10 μM) stimulation induced a contraction but did not significantly change HSP20 phosphorylation (Fig. 4). Addition of 10 μM nitroglycerin to histamine stimulated tissues induced a significant relaxation and a significant increase in HSP20 phosphorylation to 0.18 ± 0.02 mol P_i /mol HSP20. In histamine-stimulated tissues, increase in extracellular Mg^{2+} to 10 mM by addition of MgCl_2 induced a significant relaxation, but did not significantly change HSP20 phosphorylation. These data suggest that increases in HSP20 phosphorylation could have a role in nitroglycerin-induced relaxation without MRLC dephosphorylation. However, alterations in HSP20 phosphorylation cannot be responsible for high extracellular Mg^{2+} -induced relaxation without MRLC dephosphorylation.

Changes in pH affect many enzymatic processes, and the signal transduction pathway in smooth muscle is no exception. Depolarization and contractile agonist stimulation induced various degrees of intracellular acidosis in several types of intact smooth muscle tissue [20,32,33]. In isolated smooth

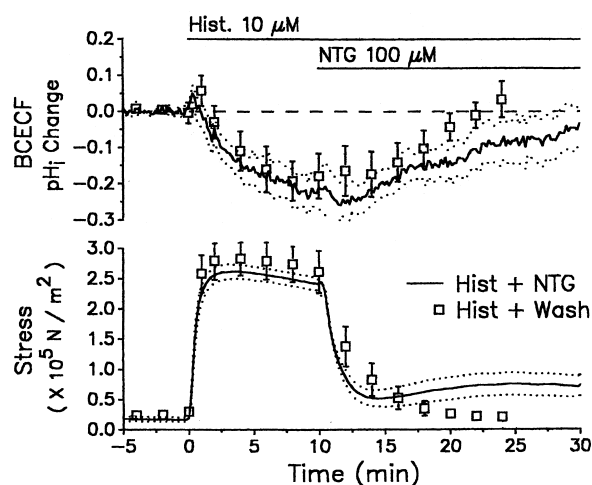


Fig. 5. pH_i during nitroglycerin-induced relaxation. The effect of nitroglycerin on histamine-induced changes in BCECF estimated pH_i (top panel) and contractile stress (bottom panel) in swine carotid media tissues. The tissues were stimulated with 10 μM histamine at 0 min and 100 μM nitroglycerin was added at 10 min (the mean is shown in a solid line with ± 1 S.E.M. in dotted lines, $n = 4$). For comparison, the effect of 10 μM histamine alone at 0 min followed by washing out histamine at 10 min is shown in open squares as mean ± 1 S.E.M.

muscle cells, changes in pH_i can alter $[\text{Ca}^{2+}]_i$ or Ca^{2+} influx/efflux [34–37]. In skinned smooth muscle, large decreases in pH_i (from 6.9 to 6.5 or 6.2) increased the $[\text{Ca}^{2+}]_i$ sensitivity of force. [14,15] These investigators used BAPTA (a Ca^{2+} chelator that is less sensitive to changes in pH than EGTA) to clamp $[\text{Ca}^{2+}]_i$ at specific levels. Therefore, their results are less susceptible to artifacts from change in pH on the EGTA buffer system. Acidosis also slowed the rate of force development by slowing changes in myosin phosphorylation.[15]

We measured pH_i in swine carotid medial tissues that were loaded with the pH -sensitive dye BCECF. Basal estimated pH_i was 7.21 ± 0.07 ($n=4$) in those tissues bathed in a physiologic saline containing the organic pH buffer MOPS. Fig. 5 shows the effect of histamine stimulation and nitroglycerin-induced relaxation on pH_i and contraction in swine carotid artery. Histamine (10 μM) stimulation induced a rapid contraction and a gradual decrease in pH_i . Addition of 100 μM nitroglycerin induced a rapid and prolonged relaxation (solid line as a running mean with dotted lines as ± 1 S.E.M.). Nitroglycerin induced a much slower increase in pH_i to near resting values. It should be noted that the BCECF signal 1–2 min after addition of histamine (when force was high) was similar to the BCECF signal 20 min after addition of nitroglycerin (when force was low). Fig. 4 also shows that washout of histamine after 10 min of contraction was also associated with a rapid relaxation and a slow increase in pH_i to near resting values, a response similar to that observed with nitroglycerin-induced relaxation. We previously found that washout of histamine was associated with reductions in Ca^{2+} to resting values [2]. These data suggest that relaxation was associated with an increase in pH_i that was similar, regardless of the mechanism inducing relaxation, i.e. whether the relaxation was caused by decreases in $[\text{Ca}^{2+}]_i$ induced by washing out histamine or processes beyond MRLC phosphorylation induced by nitroglycerin. There was no large change in pH_i that could account for relaxation without MRLC dephosphorylation.

4. Discussion

These data show that HSP20 phosphorylation was

increased by addition of nitroglycerin to histamine stimulated swine carotid artery. It is therefore possible that HSP20 phosphorylation may be involved in nitroglycerin-induced relaxation without MRLC dephosphorylation. However, relaxations induced by high extracellular magnesium, which is known to induce relaxation without MRLC dephosphorylation [11], were not associated with HSP20 phosphorylation. This result suggests that HSP20 phosphorylation is not responsible for all forms of relaxation without MRLC dephosphorylation.

The data also suggest that neither changes in caldesmon phosphorylation nor pH_i can explain relaxation without MRLC dephosphorylation in swine carotid artery. However, these data do not rule out a role for focal change in pH_i or other mechanisms that regulate caldesmon function. Further research is needed to determine: (1) whether HSP20 phosphorylation is responsible for nitroglycerin-induced relaxation; and (2) the mechanism responsible for magnesium-induced relaxation.

Finally, these data also show that histamine stimulation did not significantly alter caldesmon phosphorylation levels above that observed in unstimulated tissues. This result supports one prior report [26] that changes in caldesmon phosphorylation do not appear to correlate with contraction. Phosphorylation of caldesmon does not appear to be important in regulation of contraction in swine carotid artery. However, these data do not rule out a role for caldesmon in contraction if it is regulated by other mechanisms.

Acknowledgements

The authors would like to thank Barbara Weaver and Marcia Ripley for technical support and Dr. Len Adam for helpful discussions, the anti-caldesmon antibody, and caldesmon standards. Smithfield Co., Smithfield, VA donated the swine carotid arteries. C.M.R. is a Lucille P. Markey Scholar. Grants from the Virginia Affiliate of the American Heart Association and the Jeffress Trust supported this research.

References

- [1] A. Horowitz, C.B. Menice, R. Laporte, K.G. Morgan, *Physiol. Rev.* 76 (1996) 967–1003.
- [2] C.M. Rembold, *Am. J. Physiol. Cell Physiol.* 261 (1991) C41–C50.
- [3] N.L. McDaniel, X.-L. Chen, H.A. Singer, R.A. Murphy, C.M. Rembold, *Am. J. Physiol. Cell Physiol.* 263 (1992) C461–C467.
- [4] X.-L. Chen, C.M. Rembold, *Am. J. Physiol. Heart Circ. Physiol.* 271 (1996) H962–H968.
- [5] N.L. McDaniel, C.M. Rembold, R.A. Murphy, *Can. J. Physiol. Pharmacol.* 72 (1994) 1380–1385.
- [6] A.T. Chuang, J.D. Strauss, W.D. Steers, R.A. Murphy, *Life Sci.* 63 (1998) 185–194.
- [7] M.G. Tansey, M. Hori, H. Karaki, K.E. Kamm, J.T. Stull, *FEBS Lett.* 270 (1990) 219–221.
- [8] W.T. Gerthoffer, *J. Pharmacol. Exp. Ther.* 240 (1987) 8–15.
- [9] C.M. Rembold, *J. Physiol.* 416 (1989) 273–290.
- [10] S.S. Katoch, J.C. Rüegg, G. Pfitzer, *Pflugers Arch.* 433 (1997) 472–477.
- [11] E.K.G. D'Angelo, H.A. Singer, C.M. Rembold, *J. Clin. Invest.* 89 (1992) 1988–1994.
- [12] M. Bárány, K. Bárány, *Arch. Biochem. Biophys.* 305 (1993) 202–204.
- [13] C.M. Rembold, in: M. Barany, (Ed.), *Biochemistry of Smooth Muscle Contraction*, Academic Press, Chicago, IL, 1996, pp. 227–239.
- [14] H. Arheden, A. Arner, P. Hellstrand, *Pflugers Arch.* 413 (1989) 476–481.
- [15] J.P. Gardner, F.J.P. Diecke, *Pflugers Arch.* 412 (1988) 231–239.
- [16] A.C. Beall, K. Kato, J.R. Goldenring, H. Rasmussen, C.M. Brophy, *J. Biol. Chem.* 272 (1997) 11283–11287.
- [17] C.M. Rembold, R.A. Murphy, *Circ. Res.* 63 (1988) 593–603.
- [18] D.A. Van Riper, B.A. Weaver, J.T. Stull, C.M. Rembold, *Am. J. Physiol. Heart Circ. Physiol.* 268 (1995) H2466–H2475.
- [19] L.P. Adam, L. Milio, B. Brengle, D.R. Hathaway, *J. Mol. Cell. Cardiol.* 22 (1990) 1017–1023.
- [20] X.-L. Chen, C.M. Rembold, *Hypertension* 25 (1995) 482–489.
- [21] J. Yu, J.J. Zheng, B.Y. Ong, R. Bose, *Blood Vessels* 28 (1991) 464–474.
- [22] J.A. Lash, J.R. Sellers, D.R. Hathaway, *J. Biol. Chem.* 261 (1986) 16155–16160.
- [23] P.K. Ngai, M.P. Walsh, *J. Biol. Chem.* 259 (1984) 13656–13659.
- [24] P.K. Ngai, M.P. Walsh, *Biochem. J.* 244 (1987) 417–425.
- [25] L.P. Adam, J.R. Haeberle, D.R. Hathaway, *J. Biol. Chem.* 264 (1989) 7698–7703.
- [26] M. Bárány, E. Polyák, K. Bárány, *Arch. Biochem. Biophys.* 294 (1992) 571–578.
- [27] L.P. Adam, J.R. Haeberle, D.R. Hathaway, *Biophys. J.* 66, (1994) A198 (Abstract).
- [28] K. Kato, S. Goto, Y. Inaguma, K. Hasegawa, R. Morishita, T. Asano, *J. Biol. Chem.* 269 (1994) 15302–15309.
- [29] T. Miron, K. Vancompernelle, J. Vandekerckhove, M. Wilchek, B. Geiger, *J. Cell Biol.* 114 (1991) 255–261.
- [30] J. Guay, H. Lambert, G. Gingras-Breton, J.N. Lavoie, J. Huot, J. Landry, *J. Cell Sci.* 110 (1997) 357–368.
- [31] K.N. Bitar, M.S. Kaminski, N. Hailat, K.B. Cease, J.R. Strahler, *Biochem. Biophys. Res. Commun.* 181 (1991) 1192–1200.
- [32] C. Aalkjær, E.J. Cragoe, *J. Physiol.* 402 (1988) 391–410.
- [33] R. Bose, J. Yu, E.J. Cragoe, J. Delaive, *Prog. Clin. Biol. Res.* 327 (1990) 695–702.
- [34] B.C. Berk, T.A. Brock, M.A. Gimbrone Jr., R.W. Alexander, *J. Biol. Chem.* 262 (1987) 5065–5072.
- [35] D.R. Harder, J.A. Madden, *Pflugers Arch.* 403 (1985) 402–404.
- [36] M.S. Siskind, C.E. McCoy, A. Chobanian, J.H. Schwartz, *Am. J. Physiol.* 256 (1989) C234–C240.
- [37] A.K. Grover, C.Y. Kwan, E.E. Daniel, *Am. J. Physiol.* 244 (1983) C61–C67.